Microwave Thermal Radiometry for Detecting Cancer in Deep Human Tissues

Xunxian Xiang

Dept. of Elec. and Infor. Engrg., Huazhong University of Sci. & Tech.
Wuhan 430074 China

Abstract–In order to overcome the depth limit of detectability by a microwave radiometer for cancer, the dual Archimedes spiral Microstrip probe has to be used, which is highly effective in receiving the Microwave thermal radiation energy. The result concerning the noninvasive microwave diagnosis of cancer in deep human tissues is given in this paper.

I. FUNDAMENTALS

Microwave radiometry has been used in clinical diagnosis of breast cancer / 1, 2,3,4 / . In order to overcome the depth limit of detectability an investigation is made on the fundamentals of the probe so that the ray equation for the inhomogeneous lossless cylindrical medium is considered. Suppose the biological tissue refractive index distribution is $n = n(\rho)$. According to the Snell theory, the equation for ray $\overline{R}$ is

$$\frac{d}{dS}(n\frac{d\overline{R}}{dS}) = \nabla n \tag{1}$$

If the angle between the radius vector $\overline{\rho}$ and the ray line $\overline{R}$ at the radiation point is α, we can obtain the Abel integral equation of the first kind as follows:

$$\pi - \sin^{-1}(\frac{n_s \sin\alpha}{n_s}) = 2\int_1^{n_s \sin\alpha} \frac{-n_s \sin\alpha[\frac{1}{\rho}\frac{d\rho}{d(\rho n)}]d(\rho n)}{\sqrt{(\rho n)^2 - n_s^2 \sin^2\alpha}} \tag{2}$$

The solution is

$$n = \frac{2\sqrt{2}}{\rho^2 n_s + 2} \tag{3}$$

It can be seen that the rays can curve to a muscle with high n_m. If there is a tumor in the muscle tissue, then the rays can be concentrated on the tumor. If the thickness of all the layers are known, then the refractivity index n_i distribution and wave number $K_i = n_i k_0$ can be easily found. According to the match condition

$$n_i k_i \sin\psi_i = \text{const} \tag{4}$$

using the method of L.B. Felson / 5 / , we can make the ray path for the biological stratified medium. The larger the incidence angle ψ_{in}, the farther the refraction ray deflection from the normal line at the input point. Similarly, if the tumor in the muscle can be regarded as a microwave thermal radiation source, the ray path of tumor can be found from the wave number K_i circularity. From $n_m k_0 \sin\psi_{mc} = k_0$, we can obtain $\psi_{mc} = \sin^{-1}(1/n_m)$. The larger the n_m, the smaller the ψ_{mc}. At $\psi_m \leqslant \psi_{mc}$, the normal ray

CH3141-9/92/0000-1291$01.00 © 1992 IEEE

($\psi_m = 0$), the refraction ray ($0 < \psi_m < \psi_{mc}$) and the creep ray ($\psi_m = \psi_{mc}$) will exist on the skin surface. When detecting the tumor as an irregularity and the multiparticle microwave thermal radiation source over each detected area, it can be said that the normal ray, the refraction ray and the creep ray carry microwave thermal radiation energy (Fig. 2). As a result, we have to deal with a complex elliptical polarization wave over th skin surface. Usually, the rectangular waveguide probe /1,3,4/ filled with dielectric material can only receive a linear polarization wave. Now we have to use the dual Archimedes spiral microstrip antenna (Fig. 2), which involves a wide–band impedance matching with the human body and is highly effective for receiving elliptical polarization waves. More results of this probe will be reported at the conference.

II. MICROWAVE THERMAL RADIATION TRANSFER

The radiation transfer in layered human tissues can be considered. incident to the probe from several sources. The probe radiometric temperature T_a can be obtained:

$$T_a \approx 2\left[\frac{\Omega_{ss}}{\Omega_\rho}\left(T_s + \frac{1}{L_s}T_{ss}\right) + \frac{\Omega_{ef}}{\Omega_\rho}\frac{1}{L_s}T_f + \frac{\Omega_{sm}}{\Omega_\rho}\frac{1}{L_s L_f}T_m + \frac{\Omega_{st}}{\Omega_\rho}\frac{1}{L_s L_f L_m}T_{tu}\right] \quad (5)$$

where $\Omega\rho$ is the beam dimension of the solid angle of probe; $F_n(\theta,\varphi)$ is the normalized radiation pattern of the probe; T_s, T_f, T_m and T_{tu} are the brightness temperature of skin, fat, muscle and tumor respectively; L_s,L_f and L_m are the loss factors of skin, fat and muscle respectively, In Eq. (5), T_a is the signal containing the information about the emission characteristics of the human body. It represents a radiation power delivered by the probe to the receiver, T_{tu} represents the radiation power from the tumor.

The transfer function of the radiometer receiver is established by measuring the output voltage V as a function of the noise temperture t of a noise source connected to the probe. We can obtain the following equation:

$$t = T_c - DV \quad (6)$$

from the experimental results for measuring the brightness temperature of the equivalent muscle phantom, where T_c–the Dicke comparative temperature. Here $T_c = 323\text{K}$, $1/\text{D} = 70\text{mv}/℃$ for the new S–band microwave radiometer.

A tropic line representing the radiation transfer at the interface of a probe and the muscle model is expressed as

$$\Delta T = 1.495 + 0.995\Delta t \quad (7)$$

where Δt–hot line (simulated tumor) temperature rise difference; ΔT–measured brightness temperature difference with an S–band microwave radiometer.

III. INSTRUMENT

846S consists of a microwave thermal radiation signal extractor and an information processor. the former is made up of a dual spiral probe, a circulator (the insertion loss $\alpha_+ = 0.3\text{dB}$, the backward loss $\alpha_- \geqslant 20\text{dB}$), a Dicke modelator ($\alpha_+ = 0.3\text{dB}$, $\alpha_- \geqslant 20\text{dB}$, $f_m = 210\text{Hz}$), a reference load at a constant temperature of 323K, a low–noise amplifier ($N_f \approx 2\text{dB}$), and a square detector ($0.15\text{mv}/\mu\text{m}$); the total power gain is about 74dB. The latter consists of a low–noise AC preamplifier, a synchronous integrator, a DC amplifier, a VCO

circuit, an A / D translator, a microprocessor, and a printer. The measured brightness temperature can be printed out by the aid of a computer and is indicated on the LED display simultaneously. The main specifications of the S-band radiation balance microwave radiometer are as follows: 1. Operating frequenocies: 2.25–2.65GHz; 2. sensor: dual spiral microstrip probe with a diameter of 30mm, VSWR$<$ 2, and receiving nonlinear polarized racdiation; 3. the N_f is less than 2dB, the total microwave power gain $G_p = 74$dB; 4. temperature resolution: 0.08K with an integration time of 5 second; 5. computer-aided numerical diagnosis and simple operation; 6. detectable depth: can reach esophagus, nasopharyns, and lever.

IV. NONINVASIVE DIAGNOSIS

For nasopharyngeal cancer detection, the probe is placed on the symmetric measuring points of the face. The point-to-point measurement map for detection is shown in Fig. 3. the diagnostic critical parameters are the same as those given in P.C. Myer's definition / 1,2 / :

$$M_1 = (1/9)\left|\sum_i (\Delta T_{LR})\right| \quad (i = 1-9) \tag{8}$$

$$M_2 = \max\left\{\begin{matrix}\max(T_{Lj} - \overline{T}_L) \\ \max(T_{Rj} - \overline{T}_R)\end{matrix}\right\} \quad (j = 1-9) \tag{9}$$

We can set a critecal standard for hot points:

$$(\Delta T_{LR})_{i_{hot}} \geqslant 2.5K \tag{10}$$

where i_{hot} represents the local position numbers of these hot points. It can be seen that M_1 is most sensitive to a large-scals thermal difference, M_2 is most sensitive to a small-scale hot-spot: regardless of symmetry, i_{hot} is most sensitive to large-scale thermal discrepancy regardless of symmetry, j_{hot} is sensitive to the small-scale "hot-spot". According the the measurement data of M_1 M_2 i_{hot} and j_{hot} from 68 nasopharyngeal cancer patients (pathologically proved) and 54 other patients (not afflicted with nasopharyngeal cancer), and with the aid of the ambiguity theory. the combined criterion diagram for nasopharyngeal cancer diagnosis shown is Fig. 4. is derived. Fifty-one persons were examined by Model 846S using the criterion diagram in the Tumor Hospital of Zhongshan Medical University, Guangzhou, China, in 1988. The true positive rate was 86% while the true negative rate was 70%.

The use of an S-bamd microwave radiometer is an effective method in the screening and early diagnosis of cancer in deep tissues. This has been proved by more than 1,250 cases at 8 hospitals.

Acknowledgements

This work was supported by the National Natural Science Foundation under grant 6881006.

REFERENCES

/ 1 / A.H. Barrett, P.C. Myers and N.L. Sadowsky, "Detection of breast cancer by microwave radiometry," Radio Sci. Vol. 12, No. 6(s), p. 167,1977.

/ 2 / P.C. Myers, N.L. Sadowsky and A.H. Barrett, "Microwave thermography: Principles, methods and clinical applications," J. Microwave Power, Vol. 14, No.2, 1979.

/ 3 / A. Mamouni, F. Eliot, Y. Leroy, and Y. Moscheft, "A modified radiometer for temperature and miorowave properties measurements of biological substances, " in 7th European Microwave Conference,

1977, pp. 703–707.

/4/ K.L. Carr, A.M. El–Mahdi, and J. Shaeffer, "Dual–mode microwave system to enhance early detection of cancer, "IEEE Trans. Microwave Theory Tech., Vol. MTT 29, pp. 256–260, 1981.

/5/ L.B. Felsen, "Ray optical techniques for high–frequency fields," PPL Conference publication, 13, p. 41, 1977.

/6/ K.M. Ludeke and J. Kohler, "Microwave radiometric system for biomedical true temperature and emissivity measurements, J. Microwave Power, Vol. 18, pp. 277–288,1983.

/7/ K.L. Carr, "Microwave Radiometry: Its Importance to the Detection of Cancer," IEEE Trans. MTT–37, No. 12, pp. 1862–1869,1989.

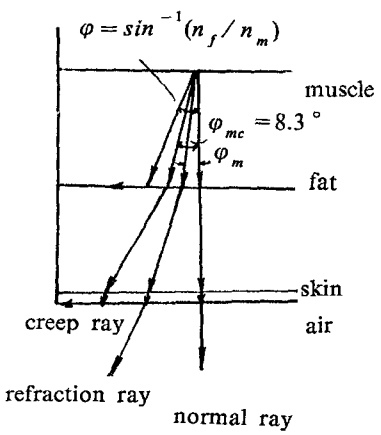

Fig.1

Microwave thermal radiation ray path of a tumor in the muscle tissue.

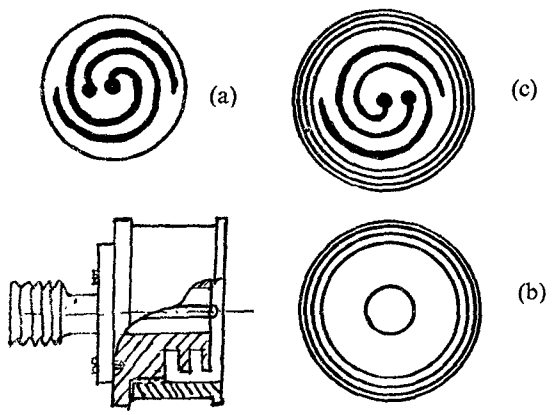

Fig. 2.

The dual Archimedes spiral microstrip probe.

a. microstrip path

b. base with check of probe

c. probe

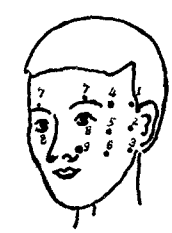

Fig. 3. The point–to–point detecting map.

nasopharyngeal cancer;

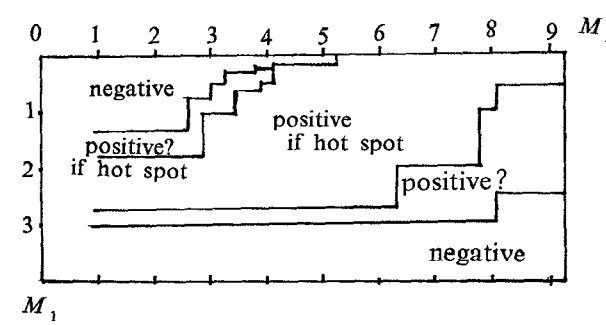

Fig. 4. The combined detecting criterion diagram of nasopharyngeal cancer.